WAVEGUIDE BEAM SPLITTERS PRODUCED ON THE BASIS OF GRADIENT MULTIMODE INTERFERENCE STRUCTURES WITH ARBITRARY POWER SPLITTING RATIO AT THE OUTPUT

Marek BŁAHUT

Institute of Physics, Silesian University of Technology, 44-100 Gliwice, ul. Krzywoustego 2, POLAND
e-mail: blahut@zeus.polsl.gliwice.pl

1. INTRODUCTION

When we excite a multimode waveguide, we can observe the effects involving the matching of input field with mode fields of the multimode waveguide, and then the interference of the produced waves. The intermode interference is accompanied by so called self-imaging effects of input field, which is exciting the multimode waveguide. As a result of these effects, the input field, which most frequently comes from a single one-mode waveguide, or from a group of one-mode waveguides, is reproduced as simple, reflected and multiple images. This phenomenon constitutes a basis for the operation of multimode interference structures (MMI). Making use of the self-imaging effects of input field, we can produce beam splitters and couplers 1xN and NxM, in which the splitting of the input field is effected within a very small area, of the order of several hundreds μm.

The development of the systems of integrated optics making use of MMI and based on step-index optical waveguides, and in particular systems based on semiconductor structures, can be observed since early 1990s [1,2]. In the works [3,4] for the first time it has been affirmed that the self-imaging effects can occur in gradient waveguides produces by ion exchange method. The work [4,5] presented optimising investigation studies involving 1x2 symmetric waveguide beam splitters produced on the basis of MMI gradient structures obtained in two basic ion exchange processes K^+ - Na^+ and Ag^+ - Na^+. The operating characteristics of 1x2 beam splitters depended on the geometry of the structure (length and width of the multimode section as well as the width of the monomode input waveguide), the parameters of technological process and polarization of light.

The works [6,7] presented waveguide 1x2 beam splitters of the arbitrary distribution of the signal at the output, made using the technology based on silicon. The configuration considered in [6] is making use of the curved MMI section, which allows obtaining an arbitrary distribution of the signal at the output. Turning the 1x2 beam splitter through a certain angle with respect to the original direction of propagation may cause problems while

designing other elements of the optoelectronic circuit. The 1x2 beam splitter system presented in [7] is making use of two MMI sections working as 3dB couplers. In the area between the MMI sections, apart from the waveguide joining them, there is a gap filled with base material. Due to the difference of refractive indexes of the waveguide core and the base, the waves reaching the second MMI section are out of phase. And consequently, the ratio of signals at the output is the function of the gap's length. However, the above solution has a weak point that is the excess loss of the structure connected with the diffraction of the field within the gap area, which is rising along with its length.

In the presented work, a new concept of the 1x2 waveguide beam splitter has been presented, on the basis of gradient multimode interference structures made with ion exchange technique Ag^{+} - Na^{+} with an arbitrary power splitting ratio at the output.

2. FUNCTIONING OF THE 1x2 BEAM SPLITTER

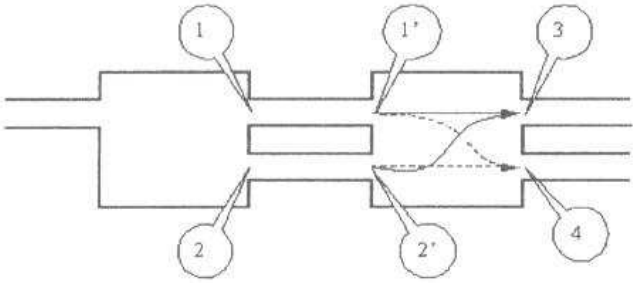

Fig.1 A block diagram of the examined 1x2 beam splitter

A block diagram of the 1x2 beam splitter is presented in Fig.1. It consists of two MMI sections working as 3dB couplers, which are joined by monomode waveguides (1) and (2). The input monomode waveguide is placed in $1/3^{rd}$ of the section's width, and the waveguides (1) and (2) as well as monomode output waveguides (3) and (4) are placed respectively in the $1/3^{rd}$ and $2/3^{rd}$ width of the multimode section. Following the theory presented in the article [2], the signal at the outputs (1) and (2) of the first section is as follows:

$$(1) = \frac{A}{\sqrt{2}} \cdot e^{j\frac{\pi}{2}} \qquad (2) = \frac{A}{\sqrt{2}}$$

where A is the amplitude of the input field. The fields at the output of the first section are out of phase by $\pi/2$. And the signal at the output of the whole unit, after the subsequent phase shift, is as follows:

$$(3) = \underset{1\to 3}{\frac{A}{\sqrt{2}}\cdot\frac{1}{\sqrt{2}}\cdot e^{j\frac{\pi}{2}}\cdot e^{j\frac{\pi}{2}}} + \underset{2\to 3}{\frac{A}{\sqrt{2}}\cdot\frac{1}{\sqrt{2}}} = \frac{A}{2}\left(e^{j\pi}+1\right) = 0$$

$$(4) = \underset{1\to 4}{\frac{A}{\sqrt{2}}\cdot\frac{1}{\sqrt{2}}\cdot e^{j\frac{\pi}{2}}} + \underset{2\to 4}{\frac{A}{\sqrt{2}}\cdot\frac{1}{\sqrt{2}}\cdot e^{j\frac{\pi}{2}}} = A\cdot e^{j\frac{\pi}{2}}$$

In consequence, we obtain a maximum signal at the output 4, and signal equal to zero at the output 3. Variable ratio of signals at the output of the 1x2 beam splitter at (3) and (4) can be obtained by changing the phases of signals propagating in the arms 1 and 2. Phase changes $\Delta\Phi$ may result from the change of the length of the arms (d_1 and d_2) or propagation constants (β_1 and β_2) of the modes propagating in waveguides 1 and 2, in compliance with the following equation:

$$\Delta\Phi = d_1\cdot\beta_1 - d_2\cdot\beta_2 \qquad (1)$$

Hence, at the inputs (1') and (2') of the second MMI section we obtain the at the outputs (3)

$$(1') = \frac{A}{\sqrt{2}}\cdot e^{j\frac{\pi}{2}+j\Delta\phi} \qquad (2') = \frac{A}{\sqrt{2}}$$

and (4) of the 1x2 beam splitter we obtain:

$$(3) = \underset{1'\to 3}{\frac{A}{\sqrt{2}}\cdot\frac{1}{\sqrt{2}}\cdot e^{j\frac{\pi}{2}}\cdot e^{j\frac{\pi}{2}+j\Delta\phi}} + \underset{2\to 3}{\frac{A}{\sqrt{2}}\cdot\frac{1}{\sqrt{2}}} = -2j\frac{A}{2}\cdot e^{j\frac{\Delta\phi}{2}}\left[\frac{e^{j\frac{\Delta\phi}{2}}-e^{-j\frac{\Delta\phi}{2}}}{2j}\right] = -jAe^{j\frac{\Delta\phi}{2}}\cdot\sin\frac{\Delta\phi}{2}$$

$$(4) = \underset{1'\to 4}{\frac{A}{\sqrt{2}}\cdot\frac{1}{\sqrt{2}}\cdot e^{j\Delta\phi+j\frac{\pi}{2}}} + \underset{2\to 4}{\frac{A}{\sqrt{2}}\cdot\frac{1}{\sqrt{2}}\cdot e^{j\frac{\pi}{2}}} = -2\frac{A}{2}\cdot e^{j\frac{\Delta\phi}{2}}\left[\frac{e^{j\frac{\Delta\phi}{2}}+e^{-j\frac{\Delta\phi}{2}}}{2}\right] = -Ae^{j\frac{\Delta\phi}{2}}\cdot\cos\frac{\Delta\phi}{2}$$

The optical power I_1 and I_2 in the output arms can be expressed by the equation:

$$(3)\quad I_1 \sim A^2\cdot\sin^2(\Delta\phi/2) \qquad (4)\quad I_2 \sim A^2\cdot\cos^2(\Delta\phi/2) \qquad (2)$$

In the configuration of the beam splitter discussed in the work, the phase shift is effected by the changes of propagation constants resulting from the difference in the width of monomode waveguides.

3. GEOMETRY OF THE 3dB MMI SECTION

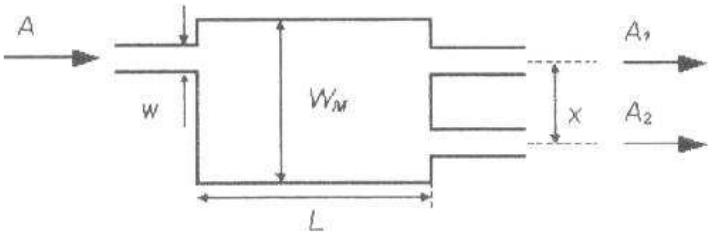

Fig.2 A diagram of the examined asymmetric MMI section

The principal element of the investigated system is the asymmetric MMI section working in the 1x2 beam splitter section as a 3dB coupler. The diagram of the investigated structure is presented in Fig.2. It consists of a monomode input waveguide obtained in the ion diffusion process through the window having the width w, placed in the 1/3rd of the window's width W_M of the multimode section of the length L, and of a pair of monomode output waveguides having the input geometry, placed in the 1/3rd and 2/3rd of the width W_M. The essential element of the gradient MMI section is a multimode waveguide made using the ion exchange method Ag+-Na+, obtained in the diffusion process of Ag+ ions through the window 16μm wide, for the diffusion depth $\sqrt{D \cdot t_D}$ =0.31 μm (D - diffusion coefficient, t_D - diffusion time), numerically calculated on the basis of a nonlinear diffusion equation [8]. For such a selected geometry and technological process parameters, as it can be seen [4] basing on the effective refractive index method, the waveguide is a multimode one for the direction congruent with the structure's width (it guides 12 modes) and a monomode waveguide for the perpendicular direction.

The propagation of the wave in the presented structure was analyzed basing on the scalar method FDBPM (*Finite Difference Beam Propagation Method*) [3].

The starting point of the FDBPM method is the Helmholtz equation in parabolic approximation. Assuming the polarization TE, we obtain the following equation:

$$-2 \cdot j \cdot k \cdot n_0 \cdot \partial E/\partial z = \partial^2 E/\partial x^2 + \partial^2 E/\partial y^2 + k^2 \cdot (n^2 - n_0^2) \cdot E \qquad (3)$$

where E(x,y,z) is describing the distribution of wave field TE, n(x,y,z) is the gradient distribution of refractive index of the investigated multimode interference structure, n_0 is the refractive index of the reference (it was accepted that $n_0 = \beta_0/k$, where β_0 is the propagation constant of the base mode of the monomode waveguide [4]. Equation (3) is solved numerically using the Alternating Direction Implicit Method [3] and Cranck-Nicholson finite difference scheme with transparent boundary conditions at the edge of the computational window. The computational window dimensions are given by l_x x l_y = 20μm x 5μm. The number of transverse grid points is 200 x 50 and the step of propagation Δz=0.5μm

The Gauss input field, after a short path of propagation, is getting matched to the monomode structure, and we observe a stable propagation of the field of the amplitude Ain until the entrance to MMI, where the distribution of input field is taking place into the fields of the modes of the multimode waveguide. After a short path of propagation, the fields in output waveguides reach the distribution of wave functions of the monomode waveguide of the amplitudes A_1 and A_2. The total excess loss α[dB] in the 1x2 beam splitter, which allows for the imaging inaccuracy of the input field in the MMI interference section and the loss involving the coupling with output waveguides is expressed by the following equation:

$$\alpha = -10 \cdot \log \frac{A_1^2 + A_2^2}{A^2} \tag{4}$$

The results of numerical simulations are presented in Figs. 3,4,5. The section MMI

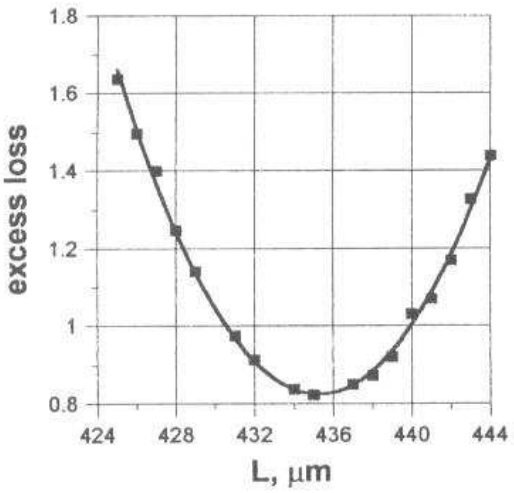

Fig.3 The dependence of excess loss in the coupler on the section length L

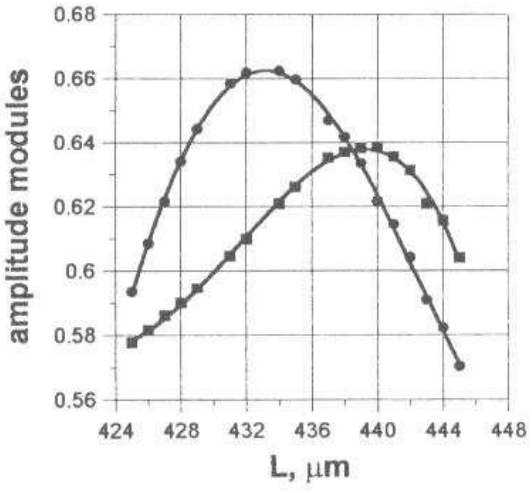

Fig.4 The dependence of the absolute values of output amplitudes A_1 and A_2 on the section length L

was excited with the field from the monomode waveguide of the width 1.20μm and the length 1050μm ensuring the matching of the Gauss beam of the wavelength λ=0.6328 μm with the field of the waveguide. With the set length between the output waveguides x=5.34μm, the length of the section was being changed within the range from 425μm to 445μm, searching for the coupling path L_{3dB} for two-fold images. Fig.3 presents the dependence of excess loss in the coupler on the length L. Minimum attenuation α=0.823 dB was obtained for the length L=435μm. The next figure, Fig.4, presents the corresponding with these changes lengths, values of output amplitude modules A_1 and A_2 (it was assumed that the amplitude of input field A=1). The conformity of output amplitudes is obtained for the propagation path L=438μm, for which the excess loss was slightly higher and equaled 0.873dB. Such a value of propagation path was accepted in further simulations as the coupling path L_{3dB} for two-fold images

4. WORKING CHARACTERISTICS OF 1x2 BEAM SPLITTER

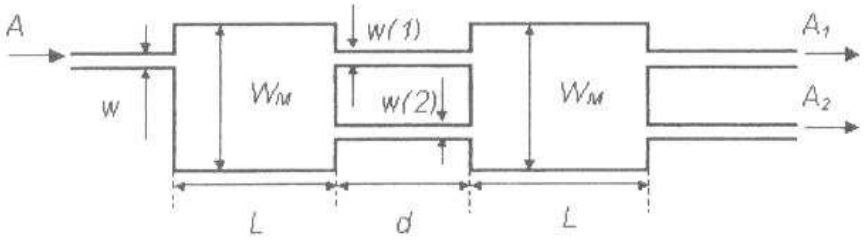

Fig.5 A diagram of 1x2 beam splitter with arbitrary power splitting ratio at the output

The diagram of 1x2 beam splitter with the arbitrary power splitting ratio at the output is presented in Fig.5. Two 3-dB MMI sections of the length L=438μm, window width W_M=16μm are joined by waveguides of different window widths $w(1)$, $w(2)$ and length d. The window widths $w(1)$, $w(2)$ are selected in the way ensuring that both waveguides stay in the monomode range. For the accepted diffusion depth 0.31μm, the width 1.3μm is the boundary of monomode range [4]. The differences of waveguides' widths result in different values of propagation constants and connected with this phase changes at the input of the second MMI section. The signals at the output will be changing according to the relations (2).

In order to carry out the tests, it was necessary to determine the optimum distance d between the sections. Fig.6 presents the dependence of excess loss on the length d for

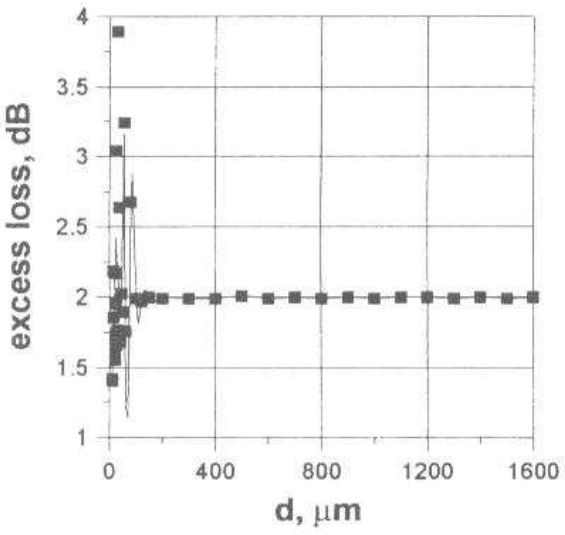

Fig.6 Excess loss as the function of the waveguide length d for $w(1) = w(2) = w =$ 1.2μm

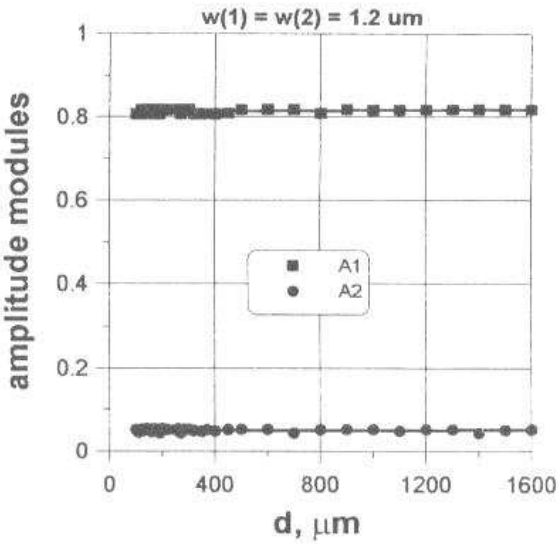

Fig.7 Absolute values of output amplitudes A_1 and A_2 as the functions of the waveguide length d for $w(1)=w(2)=w$=1.2μm

$w(1)=w(2)=w$=1.2μm. The distance was being changed within the range from 10μm to 1600μm. Up to the value of about 100μm a large dispersion of measurement points can be observed, effected by fitting the field leaving the first MMI section with the geometry of waveguides. With the increase of the distance d we observe that the attenuation is getting steady at the level α~1.7dB. In further calculations it was accepted that the minimum length of waveguides should be ~100μm. Fig.7 presents, for the same geometry of waveguides, the dependence of absolute values of output amplitudes A_1 and A_2 on the waveguide lengths d, which was being changed within the range 100μm to 1600μm. As it can be seen, the signals in both output channels are stable and are respectively A_1~0.8 and A_2~0.05 within the whole length (it was assumed that the amplitude of input field A=1).

In the next numerical simulations, the dependence of absolute values of output amplitudes A_1 and A_2 on waveguide lengths d was determined for different widths of waveguide windows $w(1)$, $w(2)$. Figures 8,9 present the characteristics for $w(1)$=1.2μm and $w(2)$=1.1μm, and for $w(1)$=1.2μm and $w(2)$=0.9μm. The window widths of the input waveguide and of output waveguides were w=1.2μm. The changes of amplitudes at the output are approximately in agreement with the relations described with equations (2). The maximum distribution of the amplitude for the characteristic presented in Fig.8 was obtained for d=220μm; A_1 has then the maximum value, i.e. 0.812, whereas the amplitude at the second

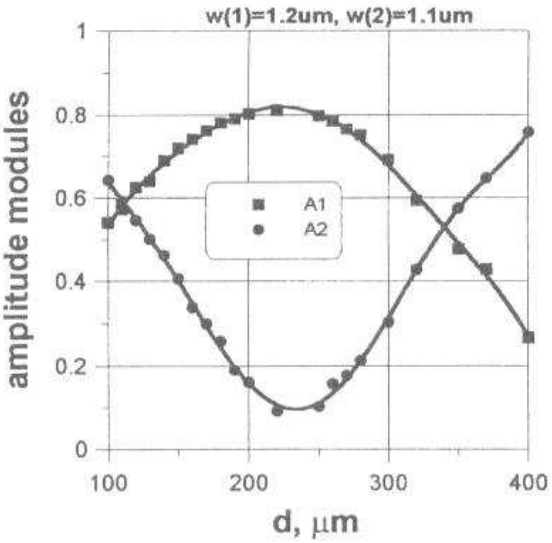

Fig.8 Absolute values of output amplitudes A_1 and A_2 as the functions of the waveguide length d for $w(1)$=1.2μm, $w(2)$=1.1μm and w =1.2μm

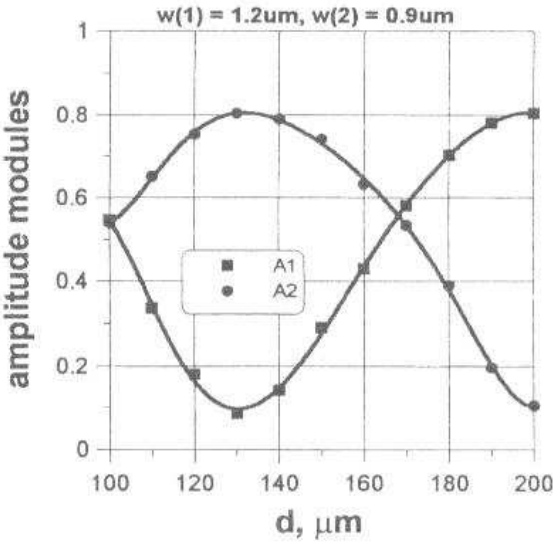

Fig.9 Absolute values of output amplitudes A_1 and A_2 as the functions of the waveguide length d for $w(1)$=1.2μm, $w(2)$=0.9μm and w =1.2μm

output reaches its minimum equal to A_2=0.09. The changing period of the amplitude is ~460μm, and average excess loss ~is sufficient to change the amplitude from the minimum value to the maximum one is 1090μm - 1320μm.

The period of the diagram from the Fig.9 is shorter and equals ~140μm. The maximum division of the amplitude was obtained for the distance d=130μm, for which A_1=0.8 and A_2=0.09.The average excess loss increased slightly as compared with the previous case, to the value 2.07dB, which is connected with higher mismatching of the size of the waveguide $w(2)$. The changes of amplitude from the minimum value to the maximum one are obtained for the structure length 1010μm - 1180μm. Making use of the dependence (1), we can estimate the changes of propagation constants corresponding with the obtained phase changes. For the characteristics from Figs. 9,10 the obtained differences of propagation constants were respectively $\Delta\beta$=0.0136μm^{-1} and $\Delta\beta$=0.0449μm^{-1}.

The characteristics presented in Figs. 10, 11, 12 involve the geometry of the structure for the window width of the input waveguide and for output waveguides w=0.9μm. Fig.10 presents the dependence of output amplitude A_1 and A_2 modules for $w(1)$=$w(2)$=w=0. 9μm on the waveguides length d, which was being changed within the range 100μm to 1600μm. The signals in both output channels are stable, and the value of total excess loss is higher than in

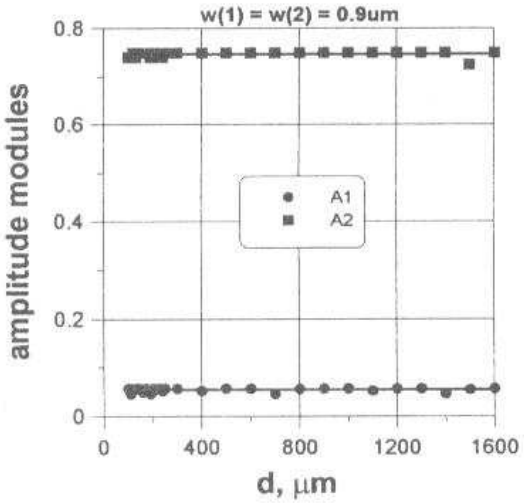

Fig.10 Absolute values of output amplitudes A_1 and A_2 as the functions of the waveguide length d for $w(1)=w(2)=w=0.9\mu m$

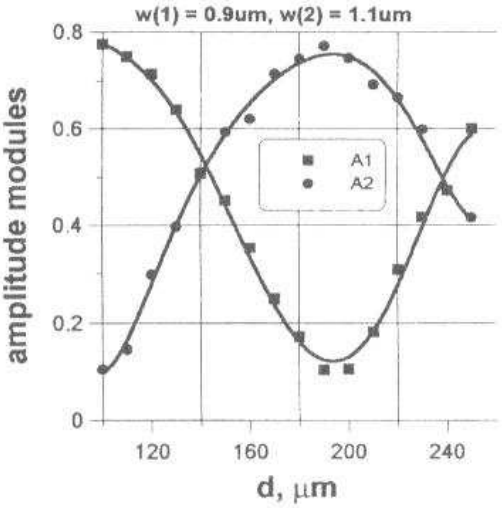

Fig.11 Absolute values of output amplitudes A_1 and A_2 as the functions of the waveguide length d for $w(1)=0.9\mu m$ $w(2)=1.1\mu m$

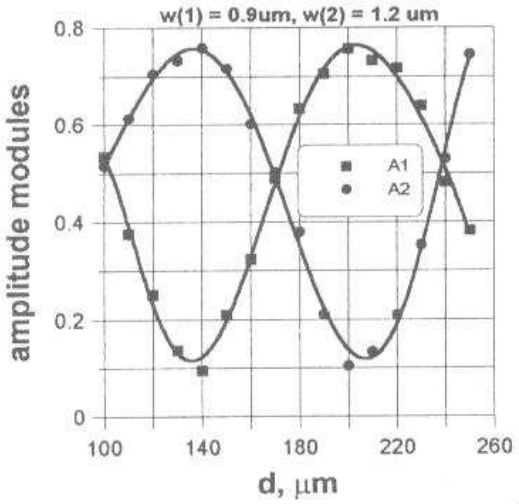

the previous case and equals 2.51dB. Figs. 11,12 present the characteristics for $w(1)=0.9\mu m$ and $w(2)=1.1\mu m$, as well as for $w(1)=0.9\mu m$ and $w(2)=1.2\mu m$. The changing period of the amplitude for the diagram from Fig.13 is ~200μm, and average excess loss ~2.57dB. For the diagram from Fig.14, which is a reversed configuration with respect to the one presented in Fig.11, the changing period of the amplitude is again ~140μm, and the average excess loss ~2.58dB. The differences of propagation constants determined basing on (1) are respectively $\Delta\beta=0.0314\mu m^{-1}$ and $\Delta\beta=0.0449\mu m^{-1}$.

5. SUMMARY

The main objective of the work involved the design and optimization studies of the waveguide 1x2 beam splitter with the arbitrary power splitting ratio at the output, which is making use of gradient multimode sections made with the application of ion exchange technique Ag^+ -Na^+ in glass. The beam splitter consists of two asymmetrical MMI sections operating as 3dB couplers joined by monomode waveguides of different width. The carried out optimization tests of the MMI section of the window width 16μm have defined the coupling path L_{3dB}=438μm for two-fold images, for which two identical images of input field are obtained with minimum excess loss ~0.87dB. Basing on the above, the operating characteristics of the 1x2 beam splitters were determined for different geometry configurations of waveguides joining the MMI section. It has been determined that the lowest excess loss is obtained for the 1x2 beam splitter having the possibly highest width of the monomode input waveguide and output waveguides. The increase of the difference of the width of waveguides joining the MMI sections results in shortening the length of 1x2 beam splitter structure, increasing at the same time excess loss connected with the size of the waveguide.

ACKNOWLEDGMENTS

This work was carried out under the Research Project of State Committee for Scientific Research, Poland (KBN), No. 8 T11B 052 18.

REFERENCES

1. L.B. Soldano, E.C. M. Pennings, J. Lightwave Technol ., LT 13, pp615-627, (1995).

2. M.Błahut, A.Opilski, Optoelectronics Rev., work accepted for publication, (2001).

3. M.Błahut, Optica Aplicata, vol 29, pp 111-125, (1999).

4. M.Błahut, Optica Aplicata, Vol.30, No.2-3, pp.401-413, (2000).

5. M.Błahut, Optoelectronics Rev., work accepted for publication, (2001).

6. Q. Lai, M. Bachman, W. Hunziker, P.A. Besse, H. Melchior , Electron. Lett, vol.32, pp. 1576-1577, (1996).

7. T. Saida, A. Himeno, M. Okuna, A.Sugita, K. Okamoto, Electron. Lett., vol.35, pp.2031-2033, (1999).